# Backbones of evolutionary history test biodiversity theory for microbes

James P. O'Dwyer[a,1], Steven W. Kembel[b], and Thomas J. Sharpton[c]

[a]Department of Plant Biology, University of Illinois, Urbana, IL 61801; [b]Département des Sciences Biologiques, Université du Québec à Montréal, Montreal, QC, Canada H2X 1Y4; and [c]Departments of Microbiology and Statistics, Oregon State University, Corvallis, OR 97331

Edited by Stephen W. Pacala, Princeton University, Princeton, NJ, and approved May 26, 2015 (received for review December 1, 2014)

**Identifying the ecological and evolutionary mechanisms that determine biological diversity is a central question in ecology. In microbial ecology, phylogenetic diversity is an increasingly common and relevant means of quantifying community diversity, particularly given the challenges in defining unambiguous species units from environmental sequence data. We explore patterns of phylogenetic diversity across multiple bacterial communities drawn from different habitats and compare these data to evolutionary trees generated using theoretical models of biodiversity. We have two central findings. First, although on finer scales the empirical trees are highly idiosyncratic, on coarse scales the backbone of these trees is simple and robust, consistent across habitats, and displays bursts of diversification dotted throughout. Second, we find that these data demonstrate a clear departure from the predictions of standard neutral theories of biodiversity and that an alternative family of generalized models provides a qualitatively better description. Together, these results lay the groundwork for a theoretical framework to connect ecological mechanisms to observed phylogenetic patterns in microbial communities.**

microbial biodiversity | macroecology | phylogeny | coalescent theory

Microorganisms play fundamental roles in the functioning of a diverse range of ecosystems, including marine and terrestrial environments as well as the human body (1), and in recent years we have had an unprecedented opportunity to measure microbial biodiversity across this range of habitats. The exploration of patterns of biodiversity has a long history in ecology, with these patterns being used to make practical predictions, such as species extinction following habitat loss (2), and also as a guide to developing ecological theory and test mechanistic hypotheses (3). However, despite the documented importance of microbial communities to human and environmental health, we currently lack the depth of ecological theory suited for microbial communities that we have for other ecological systems (4). Closing the loop between patterns and theories of microbial biodiversity is therefore a priority.

There have been two obstacles to developing a general framework linking microbial theory and data. First, ecologically meaningful species units vary for microbes and depend critically on history and environment (5). As a result, microbial biodiversity is increasingly measured using the breadth of evolutionary history spanned by a community of organisms (6). Phylogenetic measures of diversity are less well explored and less firmly connected with ecological theory than are species-based measures of diversity, and testing theories of microbial biodiversity has often still relied on the species concept (4, 7, 8), with disentangling of different mechanisms contingent on the precise species definition (5). Where phylogenetic theory has been developed (9), it has so far been difficult to draw unambiguous conclusions (10). A second problem has been that we draw heavily from our experience in the ecology of macroscopic organisms. We import theoretical frameworks that have been useful for macroscopic organisms, but microbial communities have different fundamental temporal and spatial scales and may involve new ecological and evolutionary mechanisms (11).

These difficulties point to a need for new microbial theory to be tested using phylogenetic measures of biodiversity. Here, we address this need by documenting two empirical patterns of microbial biodiversity across multiple communities and habitat types and using these as a first test for biodiversity models. The first pattern has practical applications for "upscaling" phylogenetic diversity beyond those scales we can currently sample (12), and in both cases we identify unexpected power law scaling across our communities. These echo a long history of hints of power law biodiversity scaling observed by previous studies (13, 14).

We subsequently test whether the patterns we observe can be explained by the neutral theory of biodiversity (15). Neutral theory has provided the basic null models in fields stretching from population genetics (16) and ecology (17) to cultural evolution and the social sciences (18). In common is the key assumption that selective differences are irrelevant for predicting large-scale patterns. Applying this assumption, neutral biodiversity theory has made successful predictions for species-level patterns such as species–area relationships (19) and species abundance distributions (20) and has been applied to patterns of species diversity in microbial communities (7). Here, we find that neutral models fail to explain observed patterns in microbial phylogenetic diversity, whereas another family of models, Λ-coalescents (21, 22), provides a qualitatively better description of both the scaling and topology of empirical trees. Our results suggest that standard neutral models may not provide the most useful null models for microbial communities.

## Significance

**Linking mechanism and data to explain patterns of biodiversity is a central goal in ecology. Microbial communities provide new challenges in addressing this goal, among them the potential for novel ecological mechanisms at work and also the difficulty in applying an unambiguous species concept. Patterns of evolutionary history, or phylogenetic diversity, provide an alternative framework, circumventing the need to define microbial species. We document multiple patterns of phylogenetic diversity, finding striking and unexpected similarities in these patterns across habitats, and we find that these patterns are inconsistent with neutral biodiversity theory, which has been successful in describing patterns of species diversity for macroscopic organisms. Our results suggest that a new, alternative family of models provides a better description for microbes.**

Author contributions: J.P.O., S.W.K., and T.J.S. designed research; J.P.O., S.W.K., and T.J.S. performed research; J.P.O. contributed new reagents/analytic tools; J.P.O., S.W.K., and T.J.S. analyzed data; and J.P.O., S.W.K., and T.J.S. wrote the paper.

The authors declare no conflict of interest.

This article is a PNAS Direct Submission.

Freely available online through the PNAS open access option.

[1]To whom correspondence should be addressed. Email: jodwyer@illinois.edu.

This article contains supporting information online at www.pnas.org/lookup/suppl/doi:10.1073/pnas.1419341112/-/DCSupplemental.

## Documenting Patterns of Phylogenetic Diversity

The phylogenetic diversity (PD) of a group of organisms is defined as the total branch length spanning the evolutionary tree relating these organisms. PD provides a natural alternative to taxonomic diversity (6), given that it does not rely on the ability to identify distinct microbial species and may also be correlated with functional or trait diversity. We begin by documenting two kinds of phylogenetic pattern, and we later go on to test models of biodiversity against these patterns. We first quantify the increase in phylogenetic diversity with number of individual sequences sampled from microbial communities. Across multiple habitats, we show that PD increases approximately as a power law function of sample size. Second, we explore heterogeneity in diversification rates across the same trees. To do this, we introduce a phenomenological method based on "coarse graining"—this term indicates that we will view phylogenetic trees at multiple resolutions, and this coarse-graining procedure will show that our empirical trees contain bursts of diversification throughout.

**Empirical Trees Have Consistent Scaling Behavior Across Habitats.** The relationship between the number of individuals sampled from a community and their expected phylogenetic diversity is important to understanding how much diversity may be lost from a community as organisms are removed (2, 23) and also in predicting the diversity at scales much larger than those we can sample (12). We expect phylogenetic diversity to increase with the number of individuals or sequences sampled from a community, but the rate at which it does so and whether this rate is similar across communities are unknowns. In Fig. 1 we analyze microbial communities sampled from the human gut and skin microbiomes (24), phyllosphere communities sampled on Barro Colorado Island (25), and marine environments at various latitudes drawn from the International Census of Marine Microbes (26). We choose these habitats to provide a broad range of community similarities, so that we can compare communities from two human-associated habitats, nonhuman host-associated communities and a set of non–host-associated communities. These extend earlier results in ref. 27, and further details of the samples we used can be found in *SI Appendix*, sections *A* and *B*, along with expanded plots with detailed legends. Our central conclusion is that phylogenetic diversity increases approximately as a power law with sample size across all habitats.

On the other hand, it is clear that for small samples sizes PD increases more steeply with sample size, making it difficult to interpret a power law fit. To better understand this scaling behavior, we now show how PD sampled from a community depends on an analog of the species abundance distribution termed the edge-length abundance distribution (EAD) (27), also known as a site frequency spectrum in population genetics models. We denote this distribution by a function $S(k)$, where $k$ represents the number of tips downstream of a given tree node. In effect, $k$ is the "abundance" of a clade defined by this node, described in Fig. 2. The expected phylogenetic diversity under random, binomial sampling is then given by a sum over clade sizes, $k$,

$$\mathrm{PD}(n) = \sum_k S(k)\left(1 - \left(\frac{1-n}{N}\right)^k\right), \qquad [1]$$

where total community size is $N$, and we have modeled a constant sampling effort, $n/N$. This means that every tip has an equal probability of being sampled, and the expected sample size is $n$. An example of an alternative sampling scheme would be hypergeometric sampling, where exactly $n$ tips are chosen, which produces distributions similar to binomial sampling, or clustered, negative binomial sampling (27). We note that this sampling framework is formally identical to sampling species diversity from a community with well-defined species units (28). In this case the species abundance distribution plays the same role as the EAD in Eq. **1**, and the left-hand side becomes the expected species diversity of a sample. This underlines the phylogenetic analogy between EAD and the traditional species abundance distribution.

Finally, we note that a power law behavior for the EAD, $S(k) \sim k^{-\alpha}$, then leads to an initial linear, sampling phase for sample PD for small samples (where "small" is defined in *SI Appendix*, section *C*) followed by a power law phase for larger sample sizes: $\mathrm{PD}(n) \sim n^{\alpha-1}$. In Fig. 3, we plot the EAD for each of the trees in Fig. 1 and find the EAD is approximately a power law. We fit the power law exponent using maximum likelihood, splitting each branch length into discrete segments, with grain size chosen to match the smallest branch length between any two nodes in the tree. Using these count data, we applied the maximum-likelihood method described in ref. 29, with results by habitat summarized in *SI Appendix*, Fig. S3. The exponent of the power law fit lies between $\alpha = 1.3$ and $\alpha = 1.7$, and in subsequent sections we interpret this range of values by comparison with theoretical models. Our

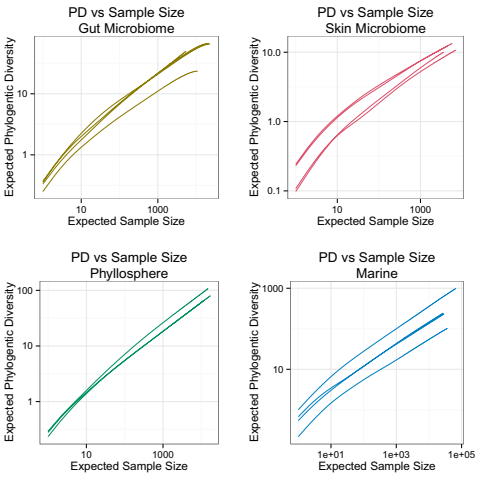


**Fig. 1.** Empirical scaling of phylogenetic diversity (PD) with sample size. PD increases with sample size approximately as a power law, for samples taken from the human gut and skin microbiomes, from phyllosphere communities in tropical forests and from marine environments at various latitudes and depths.

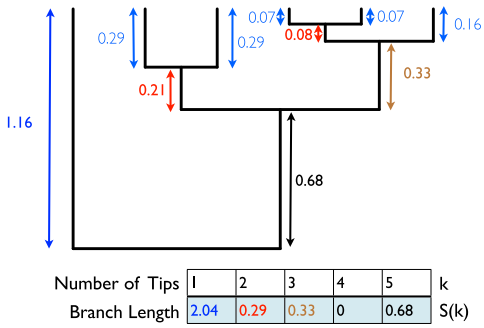


| Number of Tips | 1 | 2 | 3 | 4 | 5 | k |
|---|---|---|---|---|---|---|
| Branch Length | 2.04 | 0.29 | 0.33 | 0 | 0.68 | S(k) |

**Fig. 2.** The edge-length abundance distribution (EAD) is defined by focusing on all clades with a given, fixed number of descendant tips, $k$. For example, all tips belong to a clade with $k = 1$, and a subset of tips may also belong to clades with $k = 2$, 3, etc. For this simulated tree, there are clades with 1, 2, 3, and 5 descendant tips. For each fixed value of $k$, $S(k)$ is then the sum of the edge lengths between the node defining each clade and its immediate ancestor (27). We show these lengths in various colors for different clade sizes, $k$, with the sum for each clade size appearing in the second row of the table in the same color—one could therefore also think of this as an edge-length clade-size distribution. Finally, we note that the EAD is equivalent to the site frequency spectrum in the well-known infinite-sites population genetics model.

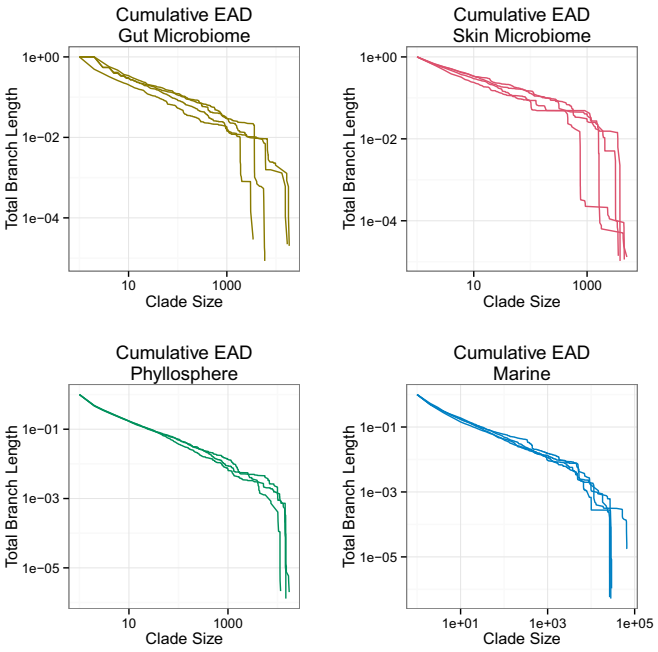


**Fig. 3.** Empirical edge-length abundance distributions follow an approximately power law distribution. The four panels show the EAD from a set of sample trees, inferred using FastTree, taken from each of four habitats: gut, skin, phyllosphere, and marine. Within each habitat multiple EADs are plotted, corresponding to different sample communities. For clarity, we have plotted the cumulative EAD, which is defined as the total branch length with greater than or equal to a given number of tips downstream. This cumulative plot can be related to the familiar idea of a rank-abundance distribution, but with $x$ and $y$ axes reversed.

central empirical observation is thus that these EADs display a similar functional form across all habitats, although we also note variation between these communities, suggesting that with more or larger samples this scaling may become informative in distinguishing between communities. In *SI Appendix*, sections *A* and *D*, we also show that our results are robust to methodology, comparing trees inferred using a rapid tree inference algorithm (FastTree) to the range of exponents arising from a maximum-likelihood tree inference algorithm (RAxML), in addition to using various systematic variations in alignment method. We find the same or very similar scaling in all cases, providing evidence that this scaling does not arise due to the bias of one particular alignment or tree-building algorithm.

**Empirical Trees Have a Simple Skeleton with Extremely Heterogeneous Branching.** We have identified a consistent scaling pattern for the EAD across multiple habitats. We now show that whereas empirical trees may be highly idiosyncratic in terms of their branching at fine phylogenetic resolutions, on coarser scales these trees have a surprisingly simple backbone structure. Our tree-inference methods are designed to resolve the nodes in our trees as finely as possible, so that two lineages always coalesce at each node. However, on coarser timescales fast bursts of branching look much like multiple lineages coalescing. We now coarse grain empirical trees by removing internal edges with length less than a fixed cutoff scale and progressively increase this cutoff, in effect making the order of branching in fast bursts indistinguishable. In Fig. 4 we show a conceptual picture of the procedure, showing that rapid bursts of branching quickly coarse grain to polytomies.

In Fig. 5 we show the effect of coarse graining one of our phyllosphere trees. We note three important features. First, there is an immediate drop in the number of internal nodes as the cutoff increases beyond the smallest branch-length segment in the tree. These smaller branch lengths are then separated from the structure of the tree on larger scales—a "skeleton" underlying the original tree. Moreover, as we remove shorter branch lengths by coarse graining we do not greatly impact branch-length weighted patterns like the EAD, and we also avoid trying to split what are presumably the most intractable polytomies to resolve, given the limits of our sequence data (30).

Previous studies have inferred evolutionary process using the distribution of internal branch lengths in a phylogeny (31). Where we now go beyond this is in identifying the structure of the coarse-grained trees defined at multiple scales. For example, following this initial collapse of nodes, the resulting distribution of polytomy sizes in the skeleton tree follows approximately a power law, a result that we would not expect a priori. Finally, these branching events are distributed deep into the tree, and not just near the tips. Taken together, this demonstrates that there is a structure of bursts of branching events in this tree, with sizes distributed self-similarly and locations distributed evenly throughout. In *SI Appendix*, section *E* we show the results of coarse graining all of our trees and we find that this resulting long-tailed distribution of polytomy sizes is typical.

## Modeling Patterns of Phylogenetic Diversity

We have identified consistent scaling behaviors for phylogenetic diversity across multiple microbial communities. Just as traditional measures of diversity like the species abundance distribution have provided useful ways to analyze theories of species biodiversity (20, 32), these aggregated phylogenetic patterns provide a first test for any theory of microbial phylogenetic diversity to explain. We now explore the hypothesis that these patterns could be generated by neutral biodiversity theory. We choose to test neutral theory, both because it has provided one of the most widely applied null models in the ecology of macroscopic organisms and therefore provides the potential for comparison between macrobial and microbial communities and because of the relative simplicity of the patterns we have uncovered. If there is a simple process underlying the simple large-scale structures we have identified, it is reasonable to think that this might be driven by the most basic model of biodiversity.

**Neutral Models Diverge from Observed Scaling of Phylogenetic Diversity.** Neutral models have been extensively used in community ecology for macroscopic organisms (15, 17, 20), as well as in the analysis of microbial communities (7, 8, 33). They have also been found in other contexts to be inconsistent with patterns on long timescales, like species ages (34, 35), and tested against a handful of summary statistics for phylogenetic trees of macroscopic organisms (36). We now test neutral predictions using the phylogenetic structure of microbial communities.

The neutral assumption is that there is no selective advantage of any individual organism over any other, and this means that we can directly translate neutral biodiversity theory into predictions for phylogenetic tree structure without using species. Neutral models typically consider total community size to be constant in time (15), and individuals divide, die, and compete symmetrically. The phylogeny of a selectively neutral group of organisms sampled from a community of fixed, large total size is then generated by the Kingman coalescent (37). We also consider a second variant, more commonly used in models of macroevolution, where a community is undergoing unregulated, exponential expansion—the Yule model (38). Here, we adapt the Yule model as a neutral model of an exponentially growing local community of microbes. Although this kind of exponential growth cannot continue indefinitely, the Yule model provides a second theoretical baseline alongside the case of constant community size.

We first focus on the scaling of the edge-length abundance distribution. The Kingman coalescent generates an approximately logarithmic increase of phylogenetic diversity with the number of tips, $n$, sampled from a tree with $N$ total tips, whereas the Yule

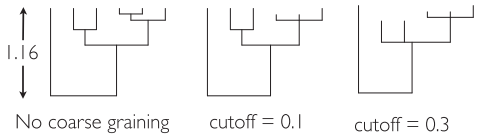


**Fig. 4.** Coarse-graining phylogenies. We coarse grain a phylogenetic tree by eliminating internal branches shorter than a given cutoff. This example takes a simulated tree and applies three different cutoffs: zero, 0.1, and 0.3.

model generates a linear increase of PD with number of tips. These two models then have corresponding behavior for the edge-length abundance distribution (39):

$$S_{\text{king}}(k) \sim \frac{1}{k}$$
$$S_{\text{yule}}(k) \sim \frac{1}{k(k-1)}. \quad [2]$$

In conclusion, neither a neutral community of constant size nor an exponentially growing community is consistent with the power law scaling of PD with sample size or the corresponding EAD we see for empirical microbial communities.

**Neutral Models Diverge from Observed Heterogeneity in Diversification Rates.** The Kingman and Yule trees fall either side of the observed EAD scaling we find for empirical communities. We now compare observed phylogenetic patterns to two alternative models of phylogenetic structure. The first is a neutral model with this more slowly changing community size, so that community size increases over time as $N(t) \sim t^{\beta}$ (defined in more detail in *SI Appendix*, section *F*). The slower increase in community size is more plausible than an exponential expansion.

The second model is the $\Lambda$ -coalescent, developed in mathematical biology (21, 22). This generalizes the Kingman coalescent (37), with the novel feature that more than two lineages can coalesce at each tree node. It has the defining rules that (*i*) the distribution of the size of these multiple coalescent events is distributed as a power law and (*ii*) these events occur throughout the tree (*SI Appendix*, section *F*). These trees have the probability of $j$ lineages coalescing at a node proportional to $\lambda(j) \sim j^{-(\gamma+1)}$, for a free parameter $\gamma$. We also note that our definition of the EAD is equivalent to the site frequency spectrum in the infinite sites model, and so we can leverage mathematical proofs relating the $\Lambda$ -coalescent tree site frequency spectra to these bursts of branching (22). By choosing a power law increase in community size over time for the neutral model and choosing an appropriate parameter $\gamma$ for the $\Lambda$ -coalescent, in both cases we can match the edge-length abundance distribution for an empirical tree:

$$S_{\text{neut}}(k) \sim k^{-1-\beta}$$
$$S_{\Lambda}(k) \sim k^{\gamma-3}. \quad [3]$$

In summary, both of these models are capable of producing the fitted scaling of a given empirical EAD by fine-tuning a single parameter.

We now explore whether the distribution of bursts of branching can distinguish between these two models. We choose model trees to have the same number of tips as the empirical tree, and we coarse grain them until they have the same number of internal nodes; this coarse graining introduces polytomies to the neutral tree and adds additional polytomies to the $\Lambda$ -coalescent. In Fig. 6, we compare the predictions of these two models to empirical tree structure. By construction, both models generate a similar EAD to that of the empirical tree. However, the neutral model does not have the same distribution of large bursts of branching found in the empirical tree, nor do bursts of branching extend deeply into the tree—they tend to be near the tips. These discrepancies are reflected across our empirical phylogenies, where we see that in all cases there are multiple peaks in the distribution of branch lengths (*SI Appendix*, Figs. S4–S7) and qualitatively fat-tailed distributions of burst sizes in between these peaks. These features do not hold for trees generated by a neutral model (*SI Appendix*, Fig. S9), suggesting that neutrality, even when combined with the hypothesis of changing community size through time, is inconsistent with the phylogenetic structure of empirical communities.

## Discussion

Evolutionary history provides a natural description for microbial diversity. The relationship between the number of individuals sampled from a community and the expected phylogenetic diversity of this sample plays a crucial and practical role both in understanding how much diversity may be lost from a community as the number of

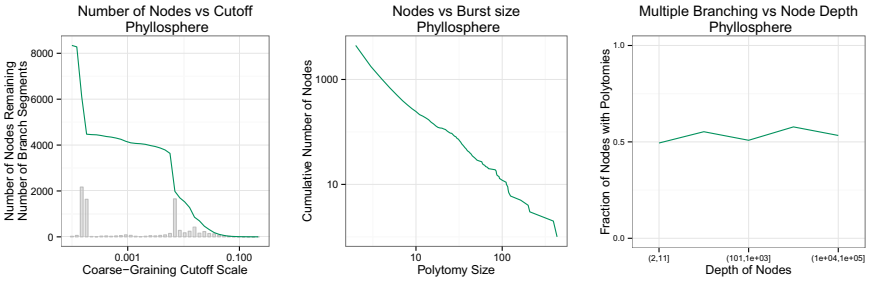


**Fig. 5.** Coarse graining an empirical phyllosphere phylogeny, sampled from leaves of angiosperm species *Inga acuminata* on Barro Colorado Island (25). *Left* shows the distribution of branch-length sizes in this tree, in the gray bars—each segment of branch length corresponds to the distance between two nodes in the tree. There are peaks in this distribution, indicating evidence of some processes acting on larger scales and, in the case of the peak of small branch lengths, potentially indicating a difficulty in resolving polytomies initially. We find that these peaks are typical across habitats (*SI Appendix*, section *E*), and this is also reflected in the solid green line (*Left*), which shows the total number of nodes as we change coarse-graining scale: Every time branch lengths shorter than a chosen scale are removed, bursts of branching collapse into "polytomies," nodes with more than two branches coalescing into them, thus reducing the total number of nodes in the tree. This first plot (*Left*) then also tells us that the choice of coarse-graining scale is not arbitrary—there are regions between the peaks where the tree structure is unchanging, and this feature remains, independent of the number of bins we choose (*SI Appendix*, section *E*). We next choose a specific cutoff scale, after coarse graining over the first peak of short branch lengths. For this coarse-grained tree, *Center* shows the cumulative distribution of the number of internal nodes as a function of polytomy size. We find that this distribution is distributed approximately as a power law for our coarse-grained phyllosphere tree. Although it is inevitable that coarse graining will generate polytomies, the form of this distribution is nontrivial. Finally, *Right* shows the fraction of nodes with multiple branches (i.e., with polytomy size $\geq 3$) as a function of the total number of tips downstream of the node, with averages calculated for logarithmically spaced bins; for this phyllosphere community, bursts of branching are distributed deep into the tree.

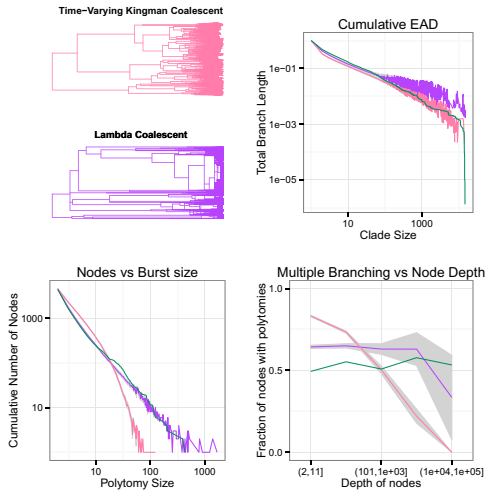


**Fig. 6.** Neutral models diverge from observed phylogenetic structure, whereas $\Lambda$ -coalescents perform qualitatively better. *Upper Left* shows example trees representing each of two one-parameter models: in pink, a neutral model, generated by a standard coalescent tree with rate of coalescence varying homogeneously over time; and in purple, a $\Lambda$ -coalescent tree, characterized by multiple coalescent events throughout the tree. *Upper Right* shows the edge-length abundance distribution for 50 instantiations of these two models, which have by construction the same scaling behavior as the phyllosphere tree (green). In contrast, *Lower Left* and *Lower Right* show that the neutral model fails to capture the fat-tailed distribution of multiple coalescent events of the coarse-grained phyllosphere tree and that these bursts of multiple branching extend much deeper into the phyllosphere tree than in the neutral model.

organisms is reduced (23) and in predicting the diversity at scales much larger than those we can sample (12). For samples taken from the human microbiome, from phyllosphere communities in tropical forests and from various marine environments, we have shown that this phylogenetic scaling is well described by sampling a power law edge-length abundance distribution, a phylogenetic analog of the well-known species abundance distribution.

Second, we introduced an approach to analyze the heterogeneity of branching events in community phylogenies and found that empirical trees have a broad distribution of bursts of branching. Our approach coarse grains over smaller branch lengths, which do not contribute substantially to branch-length weighted patterns of phylogenetic diversity, resulting in the generation of polytomies of varying sizes, and our approach therefore avoids trying to resolve these polytomies. The resulting bursts of branching are reminiscent of adaptive radiations (40–42) and may also be relevant to our understanding of power law scaling in extinction events (43, 44). These patterns also address the long-standing debate over whether evolution proceeds gradually or is punctuated by sudden changes (45). For our communities, with the caveat that we do not know their full evolutionary and ecological history, their phylogenetic trees provide quantitative evidence for a specific kind of punctuated equilibrium, characterized by power law burst sizes.

We explored whether existing biodiversity models can play a role in understanding the scaling and topological structures of empirical trees. Given the consistency of our coarse-grained tree structures, we hypothesized that selectively neutral models may provide an adequate description of this structure. In contrast, we found that real communities diverge from the predictions of neutral models. Neutral theory has predicted unrealistically large species ages (34, 35, 46), but quantitative long-term dynamics are hard to identify for many organisms, and it has been challenging to rule out neutral models using traditional snapshots of diversity like the species abundance distribution. Our results provide evidence that phylogenetic structure in microbial communities is at odds with neutral predictions.

We also found that $\Lambda$ -coalescent trees qualitatively reproduce the combination of phylogenetic scaling and bursts of branching that we see in empirical trees. What is the interpretation of these models, and what kinds of ecological and evolutionary processes might coarse grain onto these abstract tree structures? The definition of the $\Lambda$ -coalescent does not distinguish between different lineages, and so one could interpret these models as a kind of generalization of neutral theory. Indeed, these tree structures have previously been used to describe populations with skewed offspring distributions, where at the finest scales there really can be a distribution of polytomy sizes (47), but all individuals are otherwise symmetric. That is not the case here—at the finest temporal scales cell division is binary, and so the appearance of polytomies on coarse-grained scales suggests that heterogeneities between lineages persist over longer timescales. These heterogeneities could conceivably arise from fluctuations in demographic rates due to environmental stochasticity. Environmental fluctuations can produce a fat-tailed distribution of descendants, and if these fluctuations are symmetric across species, then such a model might be interpreted as a generalized, "richer" version of neutrality (48).

Recent work on fitness landscapes in population genetics provides an important clue to an alternative. One of the most successful characterizations of a fitness landscape is to assume a distribution of mutational effects. In this theoretical approach, mutations cause organisms to climb up or down a ladder of fitnesses (49–51), and the resulting models can result in many cooccurring types (52). It has recently been shown that this "clonal interference" regime generates bursts of branching on coarse-grained scales (53), with fitter lineages expanding quickly toward fixation before being overtaken by yet fitter lineages. Despite this similarity, the exponents generated in these models are more extreme than those in our bacterial phylogenies. Perhaps unsurprisingly, a ladder of fitnesses does not adequately capture the complex structure we expect in ecological communities, but it does demonstrate that selective differences can generate a power law distribution of polytomy sizes.

In combination with our work, this shows that standard neutral models and simple fitness landscapes provide two baselines for phylogenetic diversity—one generates too little heterogeneity and one too much. In between these extremes are the kinds of scaling generated by the $\Lambda$ -coalescent, where the scaling behavior is consistent with empirical trees, but we lack a definitive connection between tree structure and mechanistic hypotheses. This suggests that the path forward will need to integrate many different perspectives, bringing together the impact on phylogenetic patterns of environmental stochasticity (54–56), alongside classic macroevolutionary models describing radiations and extinctions, with models of the frequency-dependent ecological interactions and niche structures governing communities (57–62). Finally, if the observed bursts of branching do derive from the exploitation of new niches, it will also be fruitful to make direct connections with the potential mechanisms behind this exploitation. Ecological opportunities will open up after extinctions (63), but will also be driven by major events in the evolution of microbial traits, which in turn could be correlated with mechanisms such as gene transfer (64). Overall, the distribution of branch lengths in empirical trees, in combination with coarse-grained tree structure across these different scales, will provide a powerful filter for potential hypotheses.

In addition to theory development, our results also call for further empirical exploration of different communities and with larger sample sizes. We are able to identify these phenomena only over the range of scales allowed by our samples, and future studies will be needed to identify the true extent to which this scaling holds. It would also be fruitful to investigate further whether the origin of these patterns is compatible with a generalized notion of neutrality or whether the bursts we see are driven by

deterministic differences. One approach would be to identify whether the same nodes and taxa are consistently involved in bursts of diversification across different samples. Another important empirical direction will be to extend this work across a broader range of taxa. For example, power law scaling of phylogenetic diversity with sample size for angiosperm communities (65) and nonneutrality in tropical forest phylogenies (66) suggest that the patterns we see here may not be restricted to microbes. Identifying the precise similarities and differences across taxonomic groups will undoubtedly lead to a range of insights and may also require more sophisticated analytical approaches given the relatively small size of many species-level phylogenies. In general, we look forward to the development of a methodology that will incorporate and extend the patterns we have considered here, providing insight into the rules governing ecological and evolutionary processes in a range of communities.

**ACKNOWLEDGMENTS.** We acknowledge helpful comments from two anonymous reviewers, and discussions with Ryan Chisholm, Simon Dedeo, Philippe Doucet Beaupré, Jessica Green, Boris Igic, Amaury Lambert, Jay Lennon, Ken Locey, Helene Morlon, Todd Parsons, and Pedro Peres-Neto. J.P.O. acknowledges support from the Templeton World Charity Foundation Grant TWCF0079/AB47. S.W.K. was supported by the Canada Research Chairs program and the Natural Sciences and Engineering Research Council of Canada. T.J.S. acknowledges support from the Gordon & Betty Moore Foundation (Grant 3300).

1. Robinson CJ, Bohannan BJM, Young VB (2010) From structure to function: The ecology of host-associated microbial communities. *Microbiol Mol Biol Rev* 74(3):453–476.
2. Thomas CD, et al. (2004) Extinction risk from climate change. *Nature* 427(6970):145–148.
3. Rosenzweig ML (1995) *Species Diversity in Space and Time* (Cambridge Univ Press, Cambridge, UK).
4. Costello EK, Stagaman K, Dethlefsen L, Bohannan BJM, Relman DA (2012) The application of ecological theory toward an understanding of the human microbiome. *Science* 336(6086):1255–1262.
5. Hanson CA, Fuhrman JA, Horner-Devine MC, Martiny JB (2012) Beyond biogeographic patterns: Processes shaping the microbial landscape. *Nat Rev Microbiol* 10(7):497–506.
6. Faith DP (1992) Conservation evaluation and phylogenetic diversity. *Biol Conserv* 61(1):1–10.
7. Woodcock S, et al. (2007) Neutral assembly of bacterial communities. *FEMS Microbiol Ecol* 62(2):171–180.
8. Jeraldo P, et al. (2012) Quantification of the relative roles of niche and neutral processes in structuring gastrointestinal microbiomes. *Proc Natl Acad Sci USA* 109(25):9692–9698.
9. Webb CO, Ackerly DD, McPeek MA, Donoghue MJ (2002) Phylogenies and community ecology. *Annu Rev Ecol Syst* 33:475–505.
10. Mayfield MM, Levine JM (2010) Opposing effects of competitive exclusion on the phylogenetic structure of communities. *Ecol Lett* 13(9):1085–1093.
11. Morris JJ, Lenski RE, Zinser ER (2012) The Black Queen Hypothesis: Evolution of dependencies through adaptive gene loss. *MBio* 3(2):e00036-12.
12. Curtis TP, Sloan WT, Scannell JW (2002) Estimating prokaryotic diversity and its limits. *Proc Natl Acad Sci USA* 99(16):10494–10499.
13. Willis JC, Udny Yule G (1922) Some statistics of evolution and geographical distribution in plants and animals, and their significance. *Nature* 109(2728):177–179.
14. Burlando B (1993) The fractal geometry of evolution. *J Theor Biol* 163(2):161–172.
15. Hubbell SP (2001) *The Unified Neutral Theory of Biodiversity and Biogeography* (Princeton Univ Press, Princeton).
16. Kimura M (1968) Evolutionary rate at the molecular level. *Nature* 217(5129):624–626.
17. Rosindell J, Hubbell SP, Etienne RS (2011) The unified neutral theory of biodiversity and biogeography at age ten. *Trends Ecol Evol* 26(7):340–348.
18. Shennan SJ, Wilkinson JR (2001) Ceramic style change and neutral evolution: A case study from Neolithic Europe. *Am Antiq* 66:577–593.
19. Rosindell J, Cornell SJ (2007) Species-area relationships from a spatially explicit neutral model in an infinite landscape. *Ecol Lett* 10(7):586–595.
20. Volkov I, Banavar JR, Hubbell SP, Maritan A (2007) Patterns of relative species abundance in rainforests and coral reefs. *Nature* 450(7166):45–49.
21. Pitman J (1999) Coalescents with multiple collisions. *Ann Probab* 27:1870–1902.
22. Berestycki N (2009) Recent progress in coalescent theory. *Ensaios Matematicos* 16:1–193.
23. Nee S, May RM (1997) Extinction and the loss of evolutionary history. *Science* 278(5338): 692–694.
24. Peterson J, et al.; NIH HMP Working Group (2009) The NIH Human Microbiome Project. *Genome Res* 19(12):2317–2323.
25. Kembel SW, et al. (2014) Relationships between phyllosphere bacterial communities and plant functional traits in a neotropical forest. *Proc Natl Acad Sci USA* 111(38): 13715–13720.
26. Amaral-Zettler L, et al. (2010) A global census of marine microbes. *Life in the World's Oceans: Diversity, Distribution and Abundance*, ed McIntyre AD (Blackwell, Oxford), pp 223–245.
27. O'Dwyer JP, Kembel SW, Green JL (2012) Phylogenetic diversity theory sheds light on the structure of complex microbial communities. *PLoS Comput Biol* 8(12):e1002832.
28. Green JL, Plotkin JB (2007) A statistical theory for sampling species abundances. *Ecol Lett* 10(11):1037–1045.
29. Clauset A, Shalizi CR, Newman MEJ (2009) . Power-law distributions in empirical data. *SIAM Rev* 51(4):661–703.
30. Mossel M, Steel M (2005) How much can evolved characters tell us about the tree that generated them. *Mathematics of Evolution and Phylogeny*, ed Gascuel O (Oxford Univ Press, Oxford), pp 384–412.
31. Venditti C, Meade A, Pagel M (2010) Phylogenies reveal new interpretation of speciation and the Red Queen. *Nature* 463(7279):349–352.
32. Chave J, Muller-Landau HC, Levin SA (2002) Comparing classical community models: Theoretical consequences for patterns of diversity. *Am Nat* 159(1):1–23.
33. Ofițeru ID, et al. (2010) Combined niche and neutral effects in a microbial wastewater treatment community. *Proc Natl Acad Sci USA* 107(35):15345–15350.
34. Nee S (2005) The neutral theory of biodiversity: Do the numbers add up? *Funct Ecol* 19(1):173–176.
35. Chisholm RA, O'Dwyer JP (2014) Species ages in neutral biodiversity models. *Theor Popul Biol* 93:85–94.
36. Jabot F, Chave J (2009) Inferring the parameters of the neutral theory of biodiversity using phylogenetic information and implications for tropical forests. *Ecol Lett* 12(3): 239–248.
37. Kingman JFC (1982) The coalescent. *Stoch Proc Appl* 13:235–248.
38. Aldous DJ (2001) Models and descriptive statistics for phylogenetic trees, from Yule to today. *Stat Sci* 16(1):23–34.
39. Mooers A, Gascuel O, Stadler T, Li H, Steel M (2012) Branch lengths on birth-death trees and the expected loss of phylogenetic diversity. *Syst Biol* 61(2):195–203.
40. Schluter D (2000) *The Ecology of Adaptive Radiation* (Oxford Univ Press, Oxford).
41. Rainey PB, Travisano M (1998) Adaptive radiation in a heterogeneous environment. *Nature* 394(6688):69–72.
42. Martin CH, Wainwright PC (2013) Multiple fitness peaks on the adaptive landscape drive adaptive radiation in the wild. *Science* 339(6116):208–211.
43. Sneppen K, Bak P, Flyvbjerg H, Jensen MH (1995) Evolution as a self-organized critical phenomenon. *Proc Natl Acad Sci USA* 92(11):5209–5213.
44. Solé RV, Manrubia SC (1996) Extinction and self-organized criticality in a model of large-scale evolution. *Phys Rev E Stat Phys Plasmas Fluids Relat Interdiscip Topics* 54(1):R42–R45.
45. Gould SJ, Eldredge N (1977) Punctuated equilibria: The tempo and mode of evolution reconsidered. *Paleobiology* 3:115–151.
46. O'Dwyer JP, Chisholm R (2014) A mean field model for competition: From neutral ecology to the Red Queen. *Ecol Lett* 17(8):961–969.
47. Eldon B, Wakeley J (2006) Coalescent processes when the distribution of offspring number among individuals is highly skewed. *Genetics* 172(4):2621–2633.
48. Kessler DA, Shnerb NM (2014) Neutral-like abundance distributions in the presence of selection in a continuous fitness landscape. *J Theor Biol* 345:1–11.
49. Gillespie JH (1984) Molecular evolution over the mutational landscape. *Evolution* 38:1116–1129.
50. Orr HA (2005) The genetic theory of adaptation: A brief history. *Nat Rev Genet* 6(2): 119–127.
51. Kryazhimskiy S, Tkacik G, Plotkin JB (2009) The dynamics of adaptation on correlated fitness landscapes. *Proc Natl Acad Sci USA* 106(44):18638–18643.
52. Desai MM, Fisher DS, Murray AW (2007) The speed of evolution and maintenance of variation in asexual populations. *Curr Biol* 17(5):385–394.
53. Neher RA, Hallatschek O (2013) Genealogies of rapidly adapting populations. *Proc Natl Acad Sci USA* 110(2):437–442.
54. Leigh EG, Jr (1981) The average lifetime of a population in a varying environment. *J Theor Biol* 90(2):213–239.
55. Kamenev A, Meerson B, Shklovskii B (2008) How colored environmental noise affects population extinction. *Phys Rev Lett* 101(26):268103.
56. Engen S, Lande R (1996) Population dynamic models generating the lognormal species abundance distribution. *Math Biosci* 132(2):169–183.
57. Volterra V (1928) Variations and fluctuations of the number of individuals in animal species living together. *Ices J Mar Sci* 3(1):3–51.
58. MacArthur R, Levins R (1967) The limiting similarity, convergence, and divergence of coexisting species. *Am Nat* 101:377–385.
59. Tilman D (1982) *Resource Competition and Community Structure. (MPB-17)* (Princeton Univ Press, Princeton).
60. Chesson P (2000) Mechanisms of maintenance of species diversity. *Annu Rev Ecol Syst* 31:343–366.
61. Tilman D (2004) Niche tradeoffs, neutrality, and community structure: A stochastic theory of resource competition, invasion, and community assembly. *Proc Natl Acad Sci USA* 101(30):10854–10861.
62. Chisholm RA, Pacala SW (2010) Niche and neutral models predict asymptotically equivalent species abundance distributions in high-diversity ecological communities. *Proc Natl Acad Sci USA* 107(36):15821–15825.
63. Newman MEJ, Palmer RG (2003) *Modeling Extinction* (Oxford Univ Press, Oxford).
64. Dagan T, Artzy-Randrup Y, Martin W (2008) Modular networks and cumulative impact of lateral transfer in prokaryote genome evolution. *Proc Natl Acad Sci USA* 105(29):10039–10044.
65. Morlon H, et al. (2011) Spatial patterns of phylogenetic diversity. *Ecol Lett* 14(2): 141–149.
66. Wang S, Chen A, Fang J, Pacala SW (2013) Why abundant tropical tree species are phylogenetically old. *Proc Natl Acad Sci USA* 110(40):16039–16043.